International Journal of Advanced Research in Engineering and Technology (IJARET)
Volume 8, Issue 2, March - April 2017, pp. 24–41, Article ID: IJARET_08_02_004
Available online at http://www.iaeme.com/IJARET/issues.asp?JType=IJARET&VType=8&IType=2
ISSN Print: 0976-6480 and ISSN Online: 0976-6499

PERFORMANCE ASSESSMENT OF EKF AND UKF BASED DYNAMIC STATE ESTIMATORS FOR INTERMITTENT MEASUREMENT DATA IN POWER SYSTEM

Dishang D. Trivedi, Santosh C. Vora
Department of Electrical Engineering, Institute of Technology,
Nirma University, Ahmedabad, Gujarat, India

ABSTRACT

Accurate dynamic state estimation(DSE) is prime need for better monitoring and control of highly complex power system. Extended Kalman filter(EKF) and unscented Kalman filter(UKF) based algorithms are efficient tool of DSE using phasor measurement unit(PMU) based measurement data in power system. This research focuses on comparative analysis of estimation ability of EKF and UKF under the conditions of intermittent measurement data. Results recommend trade-off between duration of inconsistent measurement data and measurement data update rate to ensure converged estimation in data unavailability conditions. Simulation results are endorsed using two standard multi-machine test systems viz. WSCC 3-Generator 9-bus system and IEEE 14 bus system.

Key words: Dynamic state estimation, extended Kalman filter, measurement data update rate.

Cite this Article: Dishang D. Trivedi, Santosh C. Vora, Performance Assessment of EKF and UKF Based Dynamic State Estimators for Intermittent Measurement Data in Power System, *International Journal of Electronics and Communication Engineering and Technology*, 8(2), 2017, pp. 24–41.
http://www.iaeme.com/IJECET/issues.asp?JType=IJECET&VType=8&IType=2

1. INTRODUCTION

Energy Management Systems (EMS) plays crucial role in monitoring and control of power system. A vital part of EMS is a state estimator - a static state estimator or a dynamic state estimator. For a quasi-static power system, static state estimation (SSE) provides snapshot of steady states of power system. SSE employs telemetered measurements of instances obtained using supervisory control and data acquisition system (SCADA). SCADA based measurements have certain disadvantages e.g. measurement data with transmission delay increases measurement update time interval and introduction of noise in data. The measurements leads to cause further delay in estimation of states and hence, the SSE fails to capture dynamics of power system under transient condition. There arises need of DSE algorithm which can capture dynamics of power system. The DSE algorithm ought to be supplemented with faster measurement data, much higher than conventional SCADA system. Since it is feasible using PMUs, DSE algorithms' application to power system has gained momentum.

EKF based DSE algorithm application to power system has been widely deliberated in literature. These algorithm have capability to incorporate non-linearity in power system functions. However, EKF has limitation due to linearization error and high computation time for Jacobian calculation [1, 2, 3]. Unscented Transform based UKF offers better estimation performance as compared to EKF. The reason is linearization and Jacobian calculation are not required in UKF [2, 3].

DSE algorithms utilize measurement data from remote terminal units (RTUs). Telephone line , optical fiber, satellite signals and microwaves etc. are different means of communication channels between RTUs and EMS. Both DSE algorithms' (*viz*. EKF and UKF) performances significantly depends on data update interval and noise content in measurement [2,3,6,29]. It is noticed that UKF performs better than EKF in measurement conditions wherein exist high measurement update time interval and high measurement noise content [3]. Though recent development in measurement technology e.g. PMU has made measurement data reliable and accurate with insignificant transmission delay, a condition of complete measurement data loss to SE algorithm may arise. It could be unintentional and due to malfunction of communication link, manual error or shortcoming in communication set up [34]. Intended cyber attack could be a cause of intentional failure of communication link [7]. Errors in measurement communication of are considered to be prominent reason for power outages [4]. Hence, it seeks attention to observe the DSE algorithm's performances, if all measurement data is lost for a few cycles.

Tracking ability of EKF and UKF, along with other filters *viz.* particle filter (PF) and ensemble Kalman filter (EnKF), is presented for 100 Monte Carlo simulations using two-area four-machine system [6]. The issue of performance of EKF and UKF in case of missing measurement data is addressed in Zhou *et. al.*. Issue of measurements unavailability for duration of 1 sec is addressed by making measurements available to estimation algorithm through linear interpolation, which consequently increases effective measurement update rate [6]. With this linearly interpolated measurement data, computation time of all filters are compared and EKF offers least computation time of 4.9 s with interpolated effective measurement update time interval of 0.005 s (i.e. measurement update rate of 200 sa/s)[6]. Competitive performance of DSE algorithms *viz.* weighted least square (WLS) and EKF, under the condition of communication failure, using Kringing based load forecasting method is well presented in [5]. However, the performance of both EKF and UKF based DSE algorithms under unavailability of partial and complete measurement data remains an unaddressed issue. The authors clarifies here that partial data unavailability to algorithm means that a few data set is not available for certain duration (and no algorithmic data manipulation is performed), whereas complete unavailability of data means all the data sets have failed to update the algorithm with required sets of input information.

Addressing this, the work presented here compares and analyzes capability of EKF and UKF algorithms to estimate dynamic states *viz.* synchronous generator rotor speed, rotor angle, under partial and complete measurement data unavailability (loss) condition for a few cycles with different measurement data update rates. Results suggest desirable trade-off in selection of suitable measurement update time interval for certain duration of data unavailability for observing convergence of both filters. The possibility is explored on two multi-machine standard test systems *viz.* WSCC 3-generator, 9-bus system and IEEE 14 bus system [23, 24, 25,35].

This paper is organized as follows. Section II covers literature review. Section III takes brief glance at use of EKF and UKF for power system. Section IV presents mathematical treatment employed for DSE, procedural points considered for simulations and anomalous measurement conditions. Case studies forms Section V . Analysis and discussion comprises section VI. Concluding remarks based on presented results are presented in section VII. Reader is encouraged to refer Appendix A for detail procedural treatment of EKF and UKF algorithm.

2. LITERATURE REVIEW

Since 1970 to recent times, Kalman filter based algorithms *e.g.* EKF, UKF and their different variants evoke many researchers interests for their applications as DSE tools in power system using different measurements to estimate various dynamic states and components of power system [1], [8], [9],[12], [13], [14], [17],.[19], [20].

Reviewing impact of PMU usage on DSE algorithm's performance, it emerges that measurement data accuracy as well as measurement data update rate are critical factors. Many researchers presented improvement in estimation results of Kalman filter based algorithms using measurements of PMUs in addition to SCADA [30, 31], using PMU measurements only for multi area estimation [15] and use of discrete model DSE coordinated with load forecasting [16].

Performance of Kalman filter based algorithms (EKF and UKF) heavily depends on quality of measurement data *e.g.* content and nature of noise in measurement and availability of measurement data *e.g.* discontinuity in measurement and measurement data update rate. As core of the work in presented paper is also to analyze performance of EKF and UKF in anomalous measurement conditions, it is essential to explore researchers' efforts in this area. Nishiya *et.al.* presented a Kalman filter based algorithm for dynamic state estimation to estimate bus voltages and angles, which takes care of anomalies in bad data, change in network topology as well as sudden variation in states of network [10]. Real time estimation using robust EKF (REKF) method, which has better performance than EKF, is proposed for estimation of harmonic states of power system by [18]. With lesser number of measurements than EKF, REKF's better estimation capability under bad data condition is presented using IEEE 14 bus system [18]. For single machine infinite Bus (SMIB) system and WSCC 3-generator 9-bus test system, performance of EKF based estimator under the conditions of sudden load change and three-phase to ground fault is analyzed with anomalous measurement conditions [29]. Improved EKF using second order Euler method for EKF with multi-step prediction is offered and its performance in case of topological error, parametric error and composite error has been demonstrated with measurement update interval of 0.04 s using 16-machine 68-bus system in [21]. However, [21] suggests possibility of analyzing performance of EKF in case of measurement data unavailability. Ghahremani and Kamwa have successfully proposed EKF with unknown inputs (EKF-UI) algorithm to estimate dynamic states as well unknown inputs for SMIB system [22]. UKF performing well in comparison to WLS and EKF, for three different standard test systems, is agreeably presented in case of different transient and measurement conditions in [2].Proving UKF estimator better than EKF estimator for measurement data having different content of noises with measurement data update intervals of 0.06 s , 0.08 s and 0.1 s is well illustrated for SMIB and WSCC system in [3]. In [32] performance of EKF is deliberated in terms of error with missing measurements representation as communication packet drops. In [32] estimated state error depends on boundedness of state error covariance matrix and initial estimation error.

Literature review hints for attention towards testing estimation capability of both filters *viz.* EKF and UKF under the condition of complete unavailability of measurement data to estimation algorithm. This paper assesses ability of tracking dynamic states for both filters under the condition of few cycles of measurement data unavailability. Performance of both filters is adjudged with certain measurement data update rates.

3. BRIEF GLANCE AT EKF AND UKF FOR POWER SYSTEM

The Kalman filter based dynamic state estimation of power system is essentially based on mathematical modelling of the power system components. In power system formulations, there exists a non-linear relationship between the state and the measurements or the process itself is non-linear in nature. It is thus necessary to include these non-linearities so as to have accurate estimate of power system state variables [25]. For this reason variants of Kalman filter approach - EKF and UKF are preferably used for dynamic state estimation. Modelling requirement for power system and necessary mathematical steps for EKF and UKF are covered in literature [2, 3, 22, 26, 27, 29, 30, 31], hence not presented here. Detailed description of mathematical steps involved in EKF and UKF is presented in Appendix A.

4. TEST SYSTEMS AND SIMULATION PRELIMINARIES

4.1. State Representation and Measurement Aspects

Dynamic states to be estimated are synchronous generators rotor speeds ω_i and rotor angles δ_i. Initial states are obtained using load flow analysis. In DSE, along with accuracy of estimated results, quickness of estimation is equally important for taking critical controlling decision. Hence for mathematical modeling, 2^{nd} order classical model of synchronous generator is preferred, and related differential equations are reproduced in (1)-(2) with usual notations [23, 24]. Automatic voltage regulator(AVR) and turbine governor(TG) have not been modelled for any generator.

$$2M_i \frac{d\omega_i}{dt} = P_{m_i} - P_{g_i} - P_{d_i} \tag{1}$$

where,

M_i is inertia constant and $i = 1$ to n, $n =$ number of generators.

ω_i is actual rotor speed

P_{m_i} is assumed to be constant

P_{g_i} is electrical power generated

$P_{d_i} = D_i(\omega_i - \omega_s)/\omega_s$

ω_s is synchronous speed which is 314.1593 rad/s.

$$\frac{d\delta_i}{dt} = \frac{(\omega_i - \omega_s)}{\omega_s} \tag{2}$$

δ_i-rotor angle of i^{th} generator given in elec.rad. Frequency is taken 50 Hz in case of both test systems. Unless specified, the p.u. system of representation is used.

The dynamic state vector x is presented as,

$\mathbf{x} = [\boldsymbol{\omega}_\mathbf{i}\ \boldsymbol{\delta}_\mathbf{i}]^T$ (3)

$$\begin{bmatrix} \dot{x}_1 \\ \dot{x}_2 \end{bmatrix} = \begin{bmatrix} \frac{1}{M_i}(P_{m_i} - P_{g_i} - D_i \frac{(\omega_i - \omega_s)}{\omega_s}) \\ \frac{(\omega_i - \omega_s)}{\omega_s} \end{bmatrix}$$

so, (4)

and

$\mathbf{u} = [P_{m_i}]^T$ where, $\mathbf{u}$ is vector of input and

$$P_{g_i} = |E_i| G_{ii}^2 - \sum_{\substack{j=1 \\ j \neq i}}^{n} |E_i||E_j| (G_{ij} cos(\delta_i - \delta_j) + B_{ij} sin(\delta_i - \delta_j))$$

Where,

$G_{ii} = |Y_{ii}| cos(\theta_{ii})$ is short circuit conductance

$G_{ij} = |Y_{ij}| cos(\theta_{ij})$ is transfer conductance

$B_{ij} = |Y_{ij}| sin(\theta_{ij})$ is transfer susceptance.

Here, Y_{ii} and Y_{ij} are driving admittance and transfer admittance, respectively.

E_i is internal complex voltage of i^{th} generator behind transient reactance X'_{d_i}. It is given by $E_i = V_i + I_i.X'_{d_i}$, where V is voltage of i^{th} generator bus and I represents current injected at respective bus. Similarly vector representation of internal complex voltage is given by $\mathbf{E} = \mathbf{V} + \mathbf{I}.\mathbf{X}'_\mathbf{d}$. $\mathbf{I}$ is vector of currents injected to each bus. $\mathbf{V}$ represents complex bus voltage vector.

Current injected in each bus is derived using $\mathbf{Y}_\mathbf{exp}$ expanded nodal bus matrix (which includes internal transient reactances of generators X'_d) and is given as below : [23, 29],

$$\underbrace{\begin{bmatrix} \mathbf{Y}_{nn} & \mathbf{Y}_{nb} \\ \mathbf{Y}_{bn} & \mathbf{Y}_{bb} \end{bmatrix}}_{Y_{exp}} \begin{bmatrix} \mathbf{E} \\ \mathbf{V} \end{bmatrix} = \begin{bmatrix} \mathbf{I} \\ 0 \end{bmatrix}$$

$\mathbf{V}$ is derived by,

$$\mathbf{V} = \mathbf{R}_V \mathbf{E} = -\mathbf{Y}_{bb}^{-1}.\mathbf{Y}_{bn}\mathbf{E} \quad (5)$$

where, $\mathbf{R}_V$ is bus reconstruction matrix.

The measurements for both test systems are : 1) active and reactive power injected at generator buses; 2) voltage magnitude and angle at all buses. Measurement vectors are given by,

$$\mathbf{P}_{\mathbf{g_i}} = |\mathbf{E}_\mathbf{ii}| \mathbf{G}_\mathbf{ii}{}^2 - \sum_{\substack{j=1 \\ j \neq i}}^{n} |\mathbf{E}_\mathbf{i}||\mathbf{E}_\mathbf{j}| (\mathbf{G}_\mathbf{ij}\mathbf{cos}(\boldsymbol{\delta}_\mathbf{i} - \boldsymbol{\delta}_\mathbf{j}) + \mathbf{B}_\mathbf{ij}\mathbf{sin}(\boldsymbol{\delta}_\mathbf{i} - \boldsymbol{\delta}_\mathbf{j})) \quad (6)$$

$$\mathbf{Q_{g_i}} = |\mathbf{E_{ii}}|\mathbf{G_{ii}}^2 - \sum_{\substack{j=1 \\ j\neq i}}^{n} |\mathbf{E_i}||\mathbf{E_j}|(\mathbf{G_{ij}sin(\delta_i - \delta_j) - B_{ij}cos(\delta_i - \delta_j)}) \tag{7}$$

$$\mathbf{V_m} = |(\mathbf{R_V}.\mathbf{E})|$$

$$\boldsymbol{\theta}_\mathbf{m} = \angle(\mathbf{R_V}.\mathbf{E})$$

$m = 1,2,...b$, b is total number of buses. P_{g_i} and Q_{g_i} are injected active and reactive power at i^{th} generator bus respectively. V_m and θ_m represent voltage magnitude and voltage angle at m^{th} bus respectively.

To replicate noisy measurement conditions, measurements collected through simulation, are corrupted with white Gaussian noise having zero mean and standard deviation of 0.01 p.u.. Matrix of measurements including noise content is given by,

$$[\mathbf{y}] = \mathbf{h}(\mathbf{x},\mathbf{u},\mathbf{v}) = \begin{bmatrix} \mathbf{P_{g_i}} \\ \mathbf{Q_{g_i}} \\ \mathbf{V_m} \\ \boldsymbol{\theta}_\mathbf{m} \end{bmatrix} + \begin{bmatrix} \mathbf{v} \\ \\ \\ \\ \end{bmatrix} \tag{8}$$

h represents vector of non-linear measurement function [32, 33]. v represents vector of random white Gaussian measurement noise. Uniform process noise covariance of 0.0001 p.u. is used and initial state error covariance is 0.0001 p.u. Initial state error covariance matrix $\mathbf{P}_0$, $\mathbf{R}_k$ as measurement noise covariance matrix and $\mathbf{Q}_k$ as process noise covariance matrix are presented as,

$$\left.\begin{aligned} \mathbf{P_0} &= diag[0.0001]_{a\times a} \\ \mathbf{Q_k} &= diag[0.0001]_{a\times a} \end{aligned}\right\}, \text{a = number of states}$$

$$\mathbf{R_k} = diag[0.0001]_{d\times d}, \text{d = number of measurements}$$

For state estimation employing EKF and UKF technique, fourth order Runge - Kutta method is used to achieve better accuracy [28, 33].

4.2. Simulated Measurement Conditions

In the present paper, three measurement data update rates are chosen i.e. 50 sa/s,33 sa/s and 25 sa/s indicating measurement update time intervals of 0.02 s,0.03 s and 0.04 s respectively.Abnormal operations or failure of measurement communication devices can cause measurement data transmission interruption. Hence, data may become unavailable to DSE algorithm. Such condition is simulated at 4 s *i.e.* 2 s post three phase-to-ground fault. The measurement data are lost, partially as well as completely, for a few cycle as mentioned in Table 1.

Table 1 Summary of anomalous measurement conditions for both test systems for all three measurement update rates (50 sa/s, 33 sa/s and 25 sa/s)

Measurement data Unavailability durations	Anomalous measurement conditions for both EKF and UKF based estimator			
	Complete measurement unavailability			
	Active power	Reactive power	Bus voltage magnitude	Bus voltage angle
3, 4 and 5 cycles	X	X	X	X
	Partial measurement unavailability			
3, 4 and 5 cycles	√	√	X	X

√ - Measurement available

X - Measurement not available

Measurement data resumes after data lost duration. Test systems are analyzed for missing measurement data conditions having durations of 1 cycle to 5 cycles using EKF and UKF approaches. Only a few results are presented here for brevity.

5. CASE STUDIES

5.1. Complete Loss of Measurement Data

5.1.1. Case 1: WSCC Three Generator Nine Bus System

Performance of both the algorithms *viz.* EKF and UKF is tested for complete unavailability of measurement data using standard WSCC 3-generator 9-bus system [10, 11]. Total duration for simulation of 10 seconds.

Three phase-to-ground, metallic short, fault is simulated at t= 2 s between bus #5 and #7. Fault is cleared after 100 ms by removing the line between bus #5 and bus #7 leading to topological change (change in network configuration) of system. It subsequently changes $\mathbf{Y}_{\mathbf{bus}}$ matrix. After clearance of fault, at time t=4 s all measurement data got interrupted for time duration of 3 cycles as mentioned in Table 1. In the similar manner, algorithms are tested for measurement data lost durations of 4 cycles and 5 cycles consequently (Table 1).

Fig.1, Fig.2 and Fig.3 depict how EKF and UKF algorithms perform when measurement update time intervals are 0.02 s (50 sa/s) , 0.03 s (33 sa/s) and 0.04 s (25 sa/s), respectively.

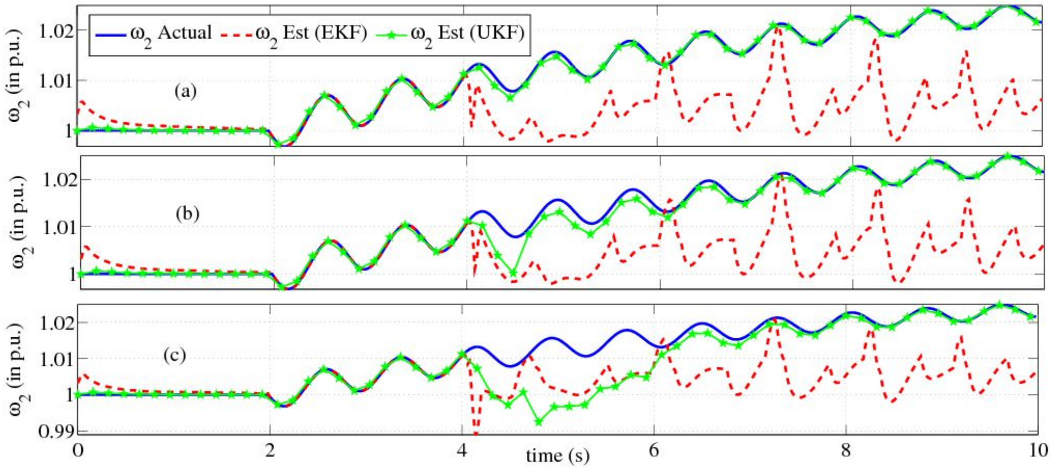

Figure 1 Performance of EKF and UKF in estimation of variations in speed of generator 2- ω_2 (WSCC system), measurement update interval of 0.02 s and all measurements missing for (a) 3 cycles, (b) 4 cycles and (c) 5 cycles duration

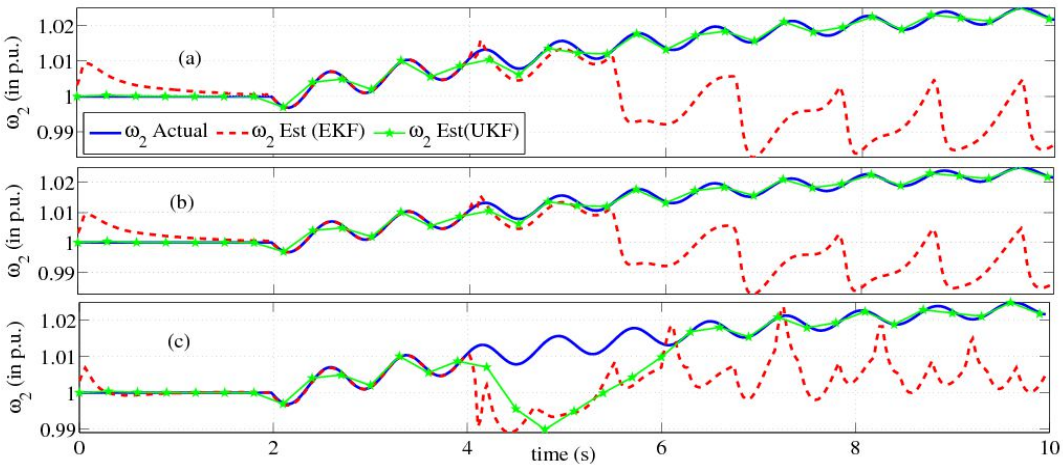

Figure 2 Performance of EKF and UKF in estimation of variations in speed of generator 2- ω_2 (WSCC system), measurement update interval of 0.03 s and all measurements missing for (a) 3 cycles, (b) 4 cycles and (c) 5 cycles duration

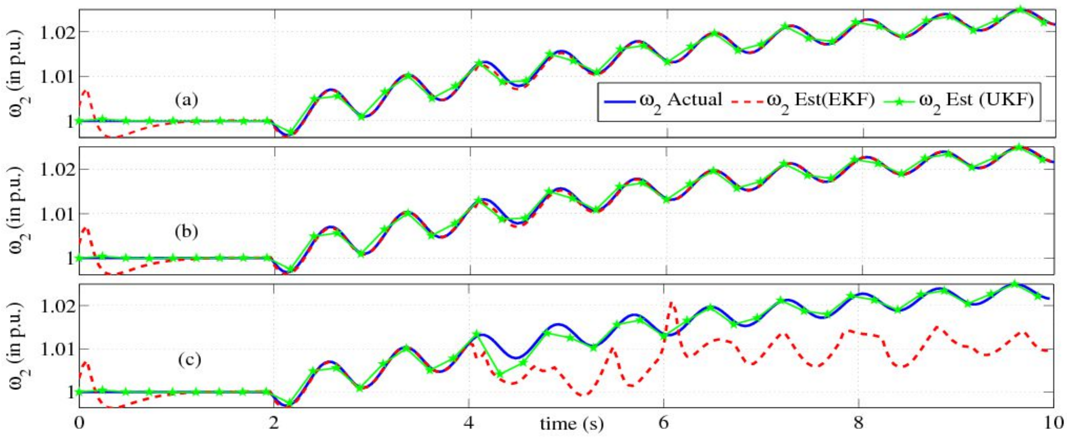

Figure 3 Performance of EKF and UKF in estimation of variations in speed of generator 2- ω_2 (WSCC system), measurement update interval of 0.04 s and all measurements missing for (a) 3 cycles, (b) 4 cycles and (c) 5 cycles duration

Keeping in view the location of fault, it is worthwhile to observe estimation of speed of generator 2 (ω_2) for EKF and UKF algorithms.

5.1.2. Case 2: IEEE 14-Bus System

The IEEE 14 bus test system [25, 35] is employed for observing proposed consideration. Similar to previous case, three phase-to-ground, metallic short fault is simulated at t = 2 s on the line between bus #4 and #5 and faulty line between bus #4 and #5 is removed by opening relevant circuit breakers after 100 ms. Necessary topological changes are used while formation of pre-fault and post-fault $\mathbf{Y_{bus}}$. Classical model of generator is considered and hence in absence of AVR and TG, system takes longer to settle to a new equilibrium condition after clearing of fault as shown in Figs. 1 - 6.

At t = 4 s,measurement data update is stopped to algorithm input for different three time periods (as shown in Table 1) and then resumes. For these missing data time durations, the tracking ability of both- EKF and UKF algorithms is observed with three measurement update rates. Total duration for observation is 20 seconds in this test case so as to check convergence possibility of both algorithms.

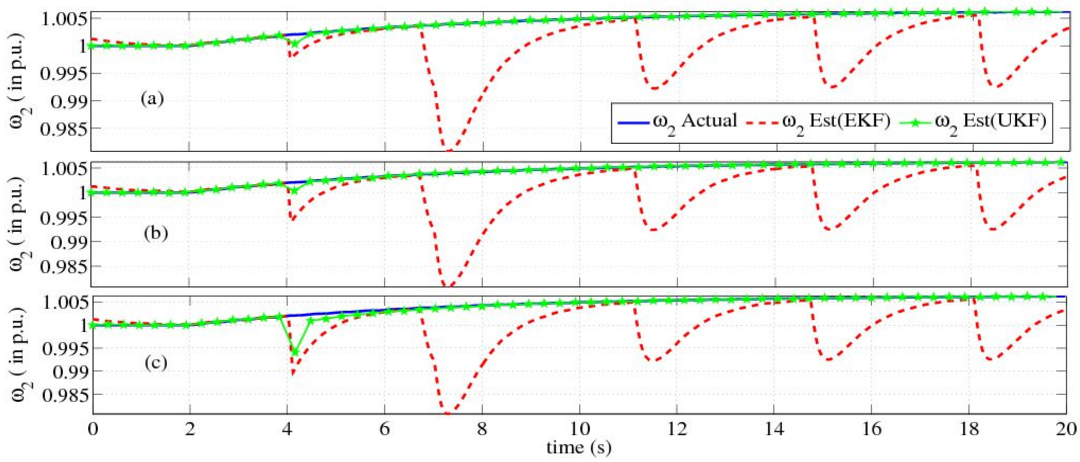

Figure 4 Performance of EKF and UKF in estimation of variations in speed of generator 2- ω_2 (IEEE 14 bus system), measurement update interval of 0.02 s and all measurements missing for (a) 3 cycles, (b) 4 cycles and (c) 5 cycles duration

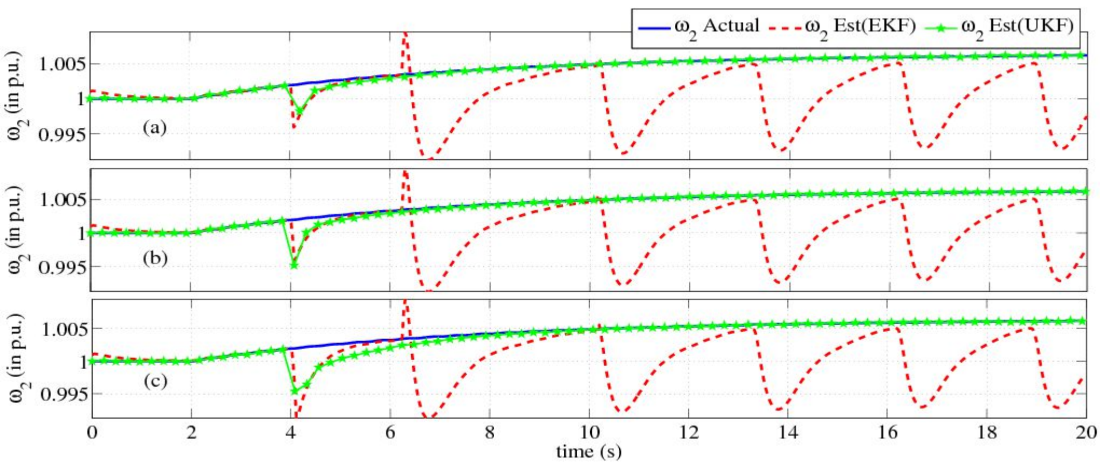

Figure 5 Performance of EKF and UKF in estimation of variations in speed of generator 2- ω_2 (IEEE 14 bus system), measurement update interval of 0.03 s and all measurements missing for (a) 3 cycles, (b) 4 cycles and (c) 5 cycles duration

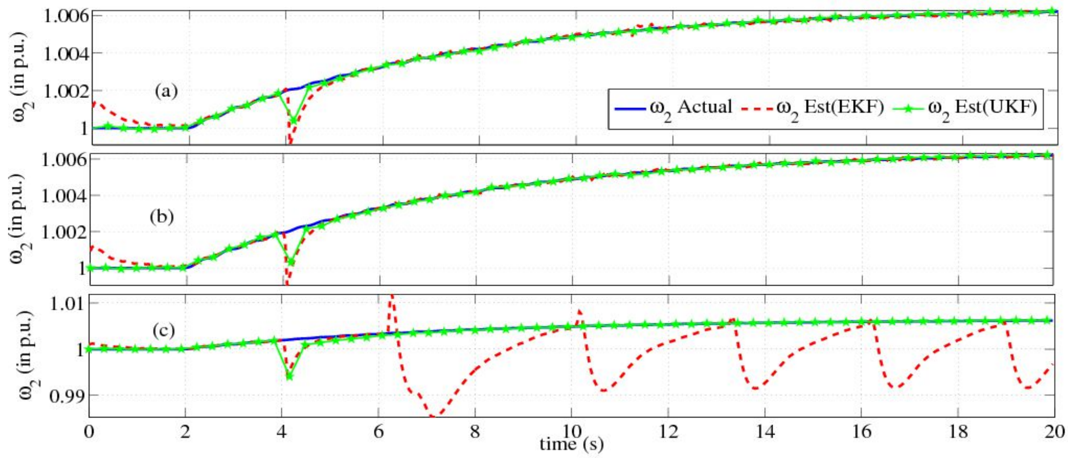

Figure 6 Performance of EKF and UKF in estimation of variations in speed of generator 2-ω_2 (IEEE 14 bus system), measurement update interval of 0.04 s and all measurements missing for (a) 3 cycles, (b) 4 cycles and (c) 5 cycles duration

Considering location of fault, only representative results of estimation of speed of generator 2 (ω_2) for both EKF and UKF algorithms are presented here.

5.2. Partial Loss of Measurement Data

As a second case, performance of EKF and UKF is analyzed for both the test systems under the condition of partial loss of measurement data i.e. out of four measurements only two measurements are unavailable. At t= 4 s, only two measurements i.e. active and reactive power are available for state estimation to both DSE algorithms as indicated in Table 1. Remaining two measurements i.e. voltage magnitude and voltage angle of buses are not provided to both estimation algorithms for the period of 3, 4 and 5 cycles. Ability of estimation is analyzed for measurement update interval of 0.02 s (update rate = 50 sa/s) which displayed divergence for all three missing measurement durations in previous case. Under these conditions with the availability of two measurements of active and reactive powers, both EKF and UKF algorithm estimates variation in speed of generator 2 (ω_2) accurately for WSCC system and IEEE 14 bus system as shown in Fig. 7 and Fig. 8 respectively . With successful estimation of one dynamic state under the condition of partial availability of measurement data, similar result of other dynamics states are not presented here.

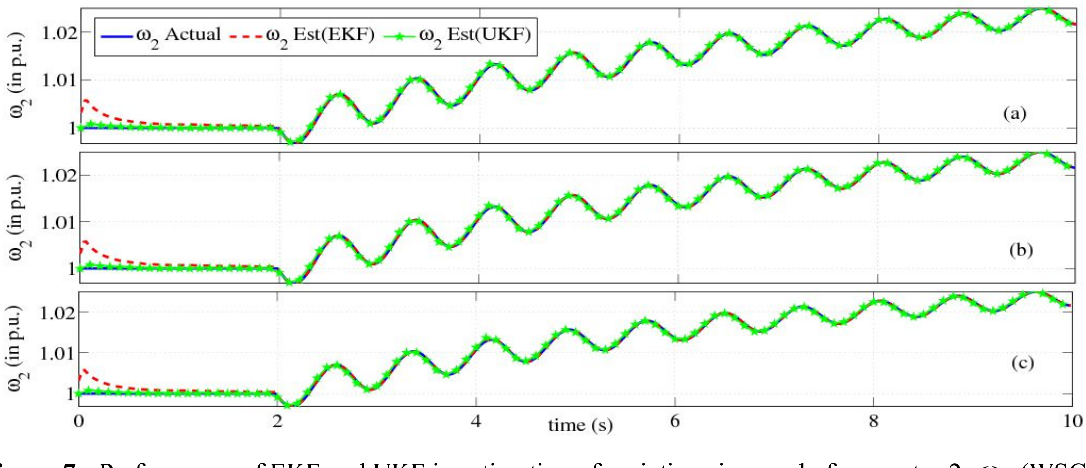

Figure 7: Performance of EKF and UKF in estimation of variations in speed of generator 2-ω_2 (WSCC system), measurement update interval of 0.02 s and two measurements missing for (a) 3 cycles, (b) 4 cycles and (c) 5 cycles duration

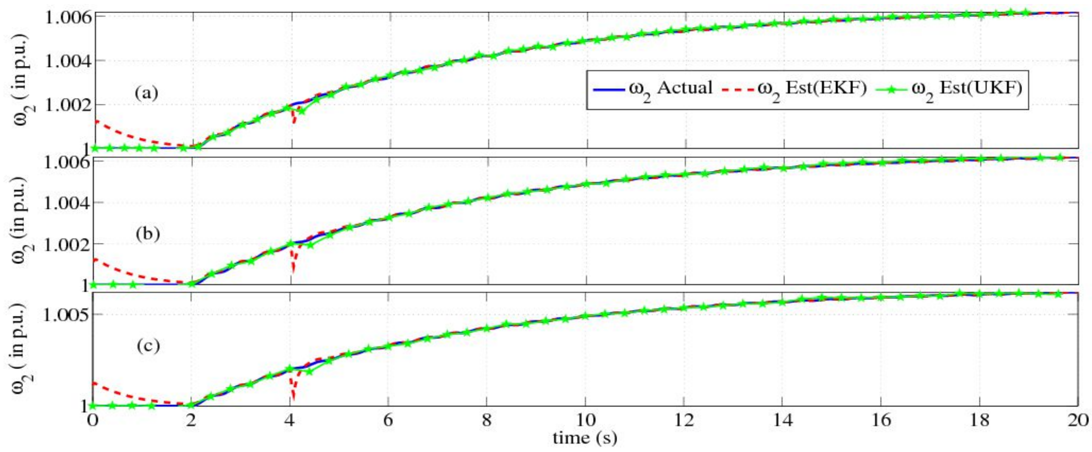

Figure 8 Performance of EKF and UKF in estimation of variations in speed of generator 2- ω_2 (IEEE 14 bus system), measurement update interval of 0.02 s and two measurements missing for (a) 3 cycles, (b) 4 cycles and (c) 5 cycles duration

6. DISCUSSION

6.1. Case 1: WSCC Test System

Ability of EKF and UKF algorithms to estimate dynamic states, post transient condition is observed under the condition of measurement data unavailability. Estimation performance is tested for data unavailablity durations of 3, 4 and 5 cycles with measurement data update rates of 50 sa/s, 33 sa/s and 25 sa/s each.

For measurement update rate of 50 sa/s (measurement time interval=0.02 s) as well as for 33 sa/s (measurement time interval=0.03 s), EKF estimator fails to track variation in speed of generator 2 (ω_2) for all three measurement data unavailability durations i.e. 3 , 4 and 5 cycles as shown in Fig.1 and Fig.2 respectively. Divergence continues though measurement data resumes. On the contrary, UKF based estimator displays efficient estimation of variations in speed of generator 2 (ω_2) for measurement update rates of 50 sa/s and 33 sa/s under all three measurement data unavailability durations as Figs. 1-2 depict.

Further in case of measurement update rate of 25 sa/s (measurement update interval= 0.04 s), EKF estimation diverges the moment data is lost (for durations of 3 cycles and 4 cycles), but converges as measurement data resumes. The estimation diverges in case of data lost duration of 5 cycles and divergence continues even after measurement data resumption as shown in Fig.3. For measurement update interval of 0.04 s, UKF estimates speed of generator 2 (ω_2) with accuracy except a momentary divergence.

Inherent nature of limited linearization and Jacobian matrix calculation in EKF cause sustained divergence once measurement data become unavailable at specific update rate. Derivation of mean and covariance of non-linear measurement functions of power system state using UT contributes to convergence after measurement data unavailability.

6.2. Case 2: IEEE 14 Bus System

Considering location of fault, results for estimation of variation in speed of generator 2(ω_2) are discussed here in detail. Fig. 4 and Fig. 5 show UKF's edge over EKF. For higher measurement update interval (0.04 s) , efficient estimation noticed for EKF in case of 3 and 4 cycles data lost duration but divergence observed when data are missing for 5 cycles duration as shown in Fig. 6. For measurement update rate of 25 sa/s, UKF based estimator accurately estimates variation in speed of generator 2(ω_2) in all three cases as displayed in Fig. 6.

It has been observed that if measurement data become unavailable for prolonged duration, however such severe condition may arise very rarely, the UKF based estimator shows divergence in case of both the multi-machine systems. Also important to note that, computational time (for 5 cycles measurement data unavailable with measurement update interval of 0.04 s) of EKF based estimator are 0.348217 s and 0.693501 s for WSCC system (total simulation time - 10 s) and IEEE 14 bus system (total simulation time - 20 s) respectively. With similar simulation conditions, the computation time of UKF based estimator are 0.17624 s and 0.353194 s for WSCC system and IEEE 14 bus system respectively. Computation time is calculated using MATLAB version *2009a* for a computer having 3.1 GHz processor, 32-bit operating system and 4 GB of RAM.Summary of results, for both the systems, is presented in Table 2.

Table 2 Comparison of EKF and UKF based estimators' performance for three measurement data unavailable conditions and measurement update time intervals

Measurement data unavailability duration	Measurement data update time interval (s) in seconds					
	EKF			UKF		
	0.02	0.03	0.04	0.02	0.03	0.04
3 cycles	*X*	*X*	√	√	√	√
4 cycles	*X*	*X*	√	√	√	√
5 cycles	*X*	*X*	*X*	√	√	√

√ - Estimation feasible

X - Estimation diverges

7. CONCLUSION

Abnormal operation or failure of measurement communication devices may cause unavailability of measurements, either partially or completely. This paper focuses on behaviour of Kalman filter based DSE algorithms *viz.* EKF and UKF under the condition in which, post to transient condition, all measurement data are unavailable for a few cycles. For EKF based estimator, normally preferred high measurement update rate, can cause divergence in case of measurement data unavailability. Application of EKF as dynamic state estimator in power system demands for trade-off between measurement data missing durations and specific measurement update rate to achieve sustained convergence. On the contrary, results shows UKF based dynamic state estimator performs better than EKF for all three durations of missing measurement conditions in combination with all three measurement data update rates. Hence, employing UKF based dynamic state estimator is more suitable than EKF to achieve continued convergence in case of infrequent condition of all measurement data unavailability.

8. APPENDIX A

A non-linear system is represented as shown in (1) [26, 27],

$$\dot{x} = \frac{d\mathbf{x}}{dt} = f(\mathbf{x}, \mathbf{u}, \mathbf{w}) \quad (1)$$

f is vector of non-linear function, x represents vector of states, u shows vector of inputs and w random white Gaussian process noise vector.

Non-linear measurement function is represented as,

$$\mathbf{y} = \mathbf{h}(\mathbf{x}, \mathbf{u}, \mathbf{v}) \tag{2}$$

where h is vector of non-linear function and v is random white Gaussian measurement noise vector. The error (ε) between actual measurement ($\mathbf{y}$) and estimated measurement ($\hat{\mathbf{y}}$) derived using state $\mathbf{x}$ is given in (3),

$$\boldsymbol{\varepsilon} = \mathbf{y} - \hat{\mathbf{y}} \tag{3}$$

8.1. Extended Kalman Filter

Step 1: Non-linear state and measurement equation shown in (1) and (2) respectively, is represented in discrete form as under:

$$\mathbf{x}_k = \mathbf{x}_{k-1} + f(\mathbf{x}_{k-1}, \mathbf{u}_{k-1}, \mathbf{w}_{k-1}) \cdot \nabla t$$

$$\mathbf{y}_k = h(\mathbf{x}_k, \mathbf{u}_k, \mathbf{v}_k)$$

$$\mathbf{w}_k \approx (0, \mathbf{Q}_k)$$

and

$$\mathbf{v}_k \approx (0, \mathbf{R}_k) \tag{4}$$

where $\mathbf{Q}_k$ is system noise covariance matrix and $\mathbf{R}_k$ is measurement noise covariance matrix.

Step 2: To initialize the filter,

$$\hat{\mathbf{x}}_0^+ = E(\mathbf{x}_0)$$

$$\mathbf{P}_0^+ = E[(\mathbf{x} - \hat{\mathbf{x}}_0^+)(\mathbf{x} - \hat{\mathbf{x}}_0^+)^T] \tag{5}$$

where $\hat{\mathbf{x}}_0^+$ is initial estimate of state matrix and $\mathbf{P}_0^+$ represents initial estimate of state error covariance matrix. The superscript + indicates *posteriori* estimate. E is expected value.

Step 3: For time update step,transition matrices for state as well as measurement vector are,

$$\mathbf{F}_{\mathbf{k-1}} = \left(\frac{\partial \mathbf{f}_{k-1}}{\partial \mathbf{x}}\right)_{\hat{\mathbf{x}}_{k-1}^+} \quad \textit{and} \quad \mathbf{L}_{\mathbf{k-1}} = \left(\frac{\partial \mathbf{f}_{k-1}}{\partial \mathbf{w}}\right)_{\hat{\mathbf{x}}_{k-1}^+} \tag{6}$$

$\mathbf{F}_{k-1}$ and $\mathbf{L}_{k-1}$ are the Jacobian of partial derivative of $\mathbf{f}$ with respect to $\mathbf{x}$ and $\mathbf{w}$, respectively. $\hat{\mathbf{x}}_{k-1}^+$ represents *posteriori* state estimate at instant $k-1$.

Time update and measurement update steps repeated at every time instant k are given below.

Step 4: **Time update**- Time update of state and error covariance matrix is done by,

$$\mathbf{P}_k^- = \mathbf{F}_{k-1}\mathbf{P}_{k-1}^+\mathbf{F}_{k-1}^T + \mathbf{L}_{k-1}\mathbf{Q}_{k-1}^+\mathbf{L}_{k-1}^T$$

$$\hat{\mathbf{x}}_k^- = f(\mathbf{x}_{k-1}^+, \mathbf{u}_{k-1}, 0) \tag{7}$$

where, − sign indicates *priori* estimate.

Step 5: Transition matrices for measurement update are,

$$\mathbf{H}_k = \left(\frac{\partial \mathbf{h}_k}{\partial \mathbf{x}}\right)_{\hat{\mathbf{x}}_k^-} \quad \textit{and} \quad \mathbf{M}_k = \left(\frac{\partial \mathbf{h}_k}{\partial \mathbf{v}}\right)_{\hat{\mathbf{x}}_k^-} \tag{8}$$

$\mathbf{H}_k$ and $\mathbf{M}_k$ are Jacobian of partial derivatives of $\mathbf{h}$ with respect to $\mathbf{x}$ and $\mathbf{v}$, respectively.

Step 6: **Measurement Update** Measurement update of state and state error covariance matrix are done by,

$$\mathbf{K}_k = \mathbf{P}_k^- \mathbf{H}_k^T (\mathbf{H}_k \mathbf{P}_k^- \mathbf{H}_k^T + \mathbf{M}_k \mathbf{R}_k \mathbf{M}_k^T)$$
$$\hat{\mathbf{x}}_k^+ = \hat{\mathbf{x}}_k^- + \mathbf{K}_k (\mathbf{y}_k - h(\mathbf{x}_k, \mathbf{v}_k))$$
$$\mathbf{P}_k^+ = (\mathbf{I} - \mathbf{K}_k \mathbf{H}_k) \mathbf{P}_k^- \quad (9)$$

where $\mathbf{K}_k$ is Kalman gain, $\hat{\mathbf{x}}_k^+$ is vector of updated state estimate and $\mathbf{P}_k^+$ is updated state error covariance matrix.

8.2. Unscented Kalman Filter

UKF is based on concept of UT which was first proposed in [1]. Although mathematical formulation and description of UKF based on UT is described in literature [1, 2, 3, 19, 27], only necessary mathematical steps for UKF based DSE are reproduced here for completeness.

First two steps, mathematical presentation and initialization of filter (*i.e.* states and state error covariance matrix) are done in same manner as shown in (4) and (5). In case of UKF, time update and measurement update are carried out as described below :

Step 3: Time update- State vector and state error covariance matrix use following steps for transition from one time instant to another.

(a) Sigma points $\tilde{\mathbf{x}}^{(r)}$ (where $r = 1,2,3...2c$) are derived as shown in (10).

$$\tilde{\mathbf{x}}^{(r1)} = \left(\sqrt{(r+\lambda)\mathbf{P}_{k-1}^+}\right)_{r1}^T$$
$$\tilde{\mathbf{x}}^{(r1+c)} = -\left(\sqrt{(r+\lambda)\mathbf{P}_{k-1}^+}\right)_{r1}^T$$
$$r1 = 1,2,3,....c \quad (10)$$

$2c$ represents total number of sigma points. The parameter λ is a scaling parameter and is defined by $\lambda = \alpha^2(a+\kappa) - a$. Value of α, that determines the spread of the sigma points around $\hat{\mathbf{x}}_{k-1}^+$, lies between $10^{-4} \le \alpha \le 1$ and second scaling parameter $\kappa = 3 - c$ or $\kappa = 0$ is preferred. Square root matrix can be approximated by $\mathbf{P} = \mathbf{A}\mathbf{A}^T$, where $\mathbf{A}$ is lower triangular matrix obtained from the Cholesky factorization of $\mathbf{P}$ [2].

Addition of sigma points $\tilde{\mathbf{x}}^{(r)}$ to recently updated *posteriori* estimate $\hat{\mathbf{x}}_{k-1}^+$ results in $\hat{\mathbf{x}}_{k-1}^r$ sigma points as shown in (11).

$$\hat{\mathbf{x}}_{k-1}^r = \hat{\mathbf{x}}_{k-1}^+ + \tilde{\mathbf{x}}^{(r)} \quad (11)$$

These sigma points are necessary for transition from $k-1^{th}$ instant to k^{th} instant.

(b) Non-linear function f is used to transform these sigma points to get vector $\hat{\mathbf{x}}_k^r$ from $\hat{\mathbf{x}}_{k-1}^r$, so

$$\hat{\mathbf{x}}_k^{(r)} = f(\hat{\mathbf{x}}_{k-1}^{(r)}, \mathbf{u}_k, t_k) \quad (12)$$

$\mathbf{u}_k$ is driving function and t_k is time at instant k.

(c) Obtaining *priori* estimate $\hat{\mathbf{x}}_k^-$, combine all $\hat{\mathbf{x}}_{k-1}^r$ using following equation,

$$\hat{\mathbf{x}}_k^- = \frac{1}{2c}\sum_{r=1}^{2c}\hat{\mathbf{x}}_k^{(r)} \quad (13)$$

(d) Evaluating *priori* state error covariance considering effect of process noise $\mathbf{Q}_{k-1}$ using

$$\hat{\mathbf{P}}_k^- = \frac{1}{2c}\sum_{r=1}^{2c}(\hat{\mathbf{x}}_k^{(r)} - \hat{\mathbf{x}}_k^-)(\hat{\mathbf{x}}_k^{(r)} - \hat{\mathbf{x}}_k^-)^T + \mathbf{Q}_{k-1} \quad (14)$$

Step 4: Measurement Update

(a) Utilizing latest time updated $\hat{\mathbf{x}}_k^-$ and $\hat{\mathbf{P}}_k^-$ to find optimum sigma points $\hat{\mathbf{x}}_k^{(r)}$ with help of following equations,

$$\begin{aligned}
\hat{\mathbf{x}}_k^r &= \hat{\mathbf{x}}_k^- + \tilde{\mathbf{x}}^{(r)} \\
\tilde{\mathbf{x}}^{(r1)} &= \left(\sqrt{(n+\lambda)\mathbf{P}_k^-}\right)_{r1}^T \\
\tilde{\mathbf{x}}^{(r1+c)} &= -\left(\sqrt{(n+\lambda)\mathbf{P}_k^-}\right)_{r1}^T
\end{aligned} \quad (15)$$

(b) Similar to time update step, for measurement update non-linear function $\mathbf{h}$ is used to transform these sigma points to get vector $\hat{\mathbf{y}}_k^r$ from $\hat{\mathbf{x}}_k^r$ such that

$$\hat{\mathbf{y}}_k^{(r)} = h(\hat{\mathbf{x}}_k^{(r)}, t_k) \quad (16)$$

(c) Obtain predicted measurement $\hat{\mathbf{y}}_k$ by combining all $\hat{\mathbf{y}}_k^r$ using following equation,

$$\hat{\mathbf{y}}_k = \frac{1}{2c}\sum_{r=1}^{2c}\hat{\mathbf{y}}_k^{(r)} \quad (17)$$

(d) Deriving measurement error covariance with effect of measurement noise $\mathbf{R}_k$ at instant k using

$$\hat{\mathbf{P}}_y^- = \frac{1}{2c}\sum_{i=1}^{2c}(\hat{\mathbf{y}}_k^{(r)} - \hat{\mathbf{y}}_k)(\hat{\mathbf{y}}_k^{(r)} - \hat{\mathbf{y}}_k)^T + \mathbf{R}_k \quad (18)$$

(e) Finding cross covariance $\hat{\mathbf{P}}_{xy}^-$

$$\hat{\mathbf{P}}_{xy}^- = \frac{1}{2a}\sum_{r=1}^{2c}(\hat{\mathbf{x}}_k^{(r)} - \hat{\mathbf{x}}_k^-)(\hat{\mathbf{y}}_k^{(r)} - \hat{\mathbf{y}}_k)^T \quad (19)$$

(f) Finally updated state estimate $\hat{\mathbf{x}}_k^+$ and state error covariance $\mathbf{P}_k^+$ are achieved using (20).

$$\begin{aligned}
\mathbf{K}_k &= \mathbf{P}_{xy}^-\mathbf{P}_y^- \\
\hat{\mathbf{x}}_k^+ &= \hat{\mathbf{x}}_k^- + \mathbf{K}_k(\mathbf{y}_k - \hat{\mathbf{y}}_k) \\
\mathbf{P}_k^+ &= \hat{\mathbf{P}}_k^- - (\mathbf{K}_k\mathbf{P}_y\mathbf{K}_k^T)
\end{aligned} \quad (20)$$

where $\mathbf{K}_k$ is Kalman gain and $\mathbf{y}_k = h(\mathbf{x}_k, \mathbf{v}_k)$.

REFERENCES

[1] Simon Julier, Jeffrey K. Uhlmann and Hugh F. Durrant-Whyte, “A new approach for filtering nonlinear systems", Proceeding of American Control Conference, Seattle WA 2,pp. 1628–1632, 1995. DOI : 10.1109/ACC.1995.529783

[2] G. Valverde and V. Terzija ,“Unscented Kalman filter for power system dynamic state estimation",IET proceedings on Gen. Trans and Dist.,Vol.5, No.1, pp.29–37, 2011. DOI: 10.1049/iet-gtd.2010.0210

[3] S Wang, W. Gao and A. P. Sakis Meliopoulos,“An alternative method for power system dynamic state estimation based on Unscented transform", IEEE Transactions on Power Systems ,Vol.27, No.2, pp.942–950, 2012. DOI: 10.1109/TPWRS.2011.2175255

[4] Z. Xie, G. Manimaran, V. Vittal and A. G. Phadke, “An information architecture for future power systems and its reliability analysis ", IEEE trans. on Power Syst., Vol.17, no. 3, pp. 857-863, 2002.

[5] Chaojun Gu and Panida Jirutitijaroen,“Dynamic state estimation under communication failure using Kriging based bus load forecasting", IEEE trans. on Power system , Vol.30, No.6, pp. 2831–2840, 2015. DOI: 10.1109/TPWRS-01138-2013.

[6] Ning Zhou, Da Meng, Zhenyu Huang and Greg Welch, “Dynamic State Estimation of a Synchronous Machine Using PMU Data : A Comparative Study", IEEE Trans. on Smart grid. Vol.6,No.1,pp.450-460, 2015. DOI: 10.1109/TSG.2014.2345698.

[7] [7] S. Sridhar, A. Hahn and M. Govindarasu, “Cyber-physical system security for the electric power grid", Proceedings IEEE,Vol.100,No.1,pp.210-224,2012.

[8] A. Debs and R. Larson, “A dynamic estimator for tracking the state of power system", IEEE Trans. Power Apparatus and systems,PAS, Vol.89, No.7, pp. 1670–1678, 1970. DOI: 10.1109/TPAS.1970.292822

[9] W. Miller and J.B.Lewis, “Dynamic state estimation in power systems", IEEE Transactions Automatic control, Vol.16, No.6, pp. 841–846, 1971. DOI: 10.1109/TAC.1971.1099844

[10] K. Nishiya, J. Hasegawa and T. Koike, “Dynamic state estimation including anomaly detection and identification for power system", IEE Proceedings Gen. Trans. and Dist., Vol.129, No.5, pp. 192–198, 1982. DOI: 10.1049/ip-c.1982.0032

[11] A. Leite da Silva, M. Do Coutto Filho and J. F. Queiroz, “State forecasting in electric power systems",IEE Proceedings on Gen. Trans. and Dist., Vol.130, No.5, pp.237–244, 1983. DOI: 10.1049/ip-c.1983.0046

[12] J. K. Mandal, A. K. Sinha and L. Roy, “Incorporating nonlinearities of measurement function in power system dynamic state estimation", IEE Proceedings on Gen. Trans. Dist., Vol.142, No.3,pp.289-296,1995. DOI: 10.1049/ip-gtd:19951715

[13] J. K. Mandal and A.K. Sinha, “Hierarchical Dynamic state estimation incorporating measurement function non-linearities", International Journal of Electrical Power and Energy System, Vol.19, No.1, pp. 57–67,1996.

[14] B. Subudhi, P.K. Ray, S.R. Mohanty, A.M. Panda, “A comparative study on different power system frequency estimation techniques", International Journal of Automation and Control, Vol. 3, No.2/3 pp. 202 - 215, 2009. DOI: 10.1504/IJAAC.2009.025242.

[15] Arash Vahidnia, Gerard Ledwich, Edward Palmer and Arindam Ghosh, “Dynamic equivalent state estimation for multi-area power systems with synchronized phasor measurement units", International journal of Electric Power Systems Research, Vol.96, pp.170–176, 2013.

[16] E. A. Blood, B. Krogh and M. Ilic, "Electric power system static state estimation through kalman filtering and load forecasting", Proceeding of IEEE Power and energy society general meeting-Conversion and Delivery of Electrical energy in the 21st century , pp.1–6,2008. DOI: 10.1109/PES.2008.4596742

[17] Lingling Fan and Yasser Wehbe, "Extended Kalman filtering based real-time dynamic state and parameter estimation using PMU data", Electric Power Systems Research, Vol.103, pp.168–177, 2013.

[18] Ashwani Kumar, Biswaroop Das and Jaydev Sharma, "Robust Dynamic State Estimation of Power System Harmonics", International Journal of Electrical Power and Energy Systems , Vol.28, pp. 65–74, 2006.

[19] P. Regulski and V. Terzija,"Estimation of frequency and fundamental power components using unscented Kalman filter", IEEE Transactions Instrumentation and Measurement , Vol. 61, No. 4,pp.952–962,2012. DOI: 10.1109/TIM.2011.2179342

[20] Miao Huanga,Wenyuan Li b and Wei Yana, "Estimating parameters of synchronous generators using square-root unscented Kalman filter" International journal of Electric Power Systems Research, Vol.80, pp.1137–1144, 2010.

[21] Zhenyu Huang, Kevin Schneider, Ning Zhou and Jarek Nieplocha,"Estimating power system dynamic states using extended Kalman filter", IEEE PES General meeting : conference and exposition, pp.1–5, 2014. DOI: 10.1109/PESGM.2014.6939934

[22] E. Ghaheramani and I. Kamwa, "Dynamic state estimation in power system by applying the extended Kalman filter with unknown inputs to phasor measurements", IEEE Transactions Power Systems, Vol.26, No. 4, pp. 2556–2566, 2011. DOI: 10.1109/TPWRS.2011.2145396.

[23] P.M. Anderson and A.A. Fouad, "Power system control and stability", 2nd Ed.,IEEE Press, Wiley India Pvt. Ltd., India, 2008.

[24] P.W. Sauer and M. A. Pai, "Power System Dynamics and Stability",Prentice Hall,India, 1998.

[25] M. A. Pai,"Computer techniques in power system analysis" ,Tata McGraw Hill,India, 1979.

[26] G. Welch and G. Bishop ,"An introduction to the Kalman filter", TR 95-041, Dept. of Computer Science, Uni. of North Carolina at Chapel Hill, 2004.

[27] D.Simon, "Optimal State Estimation : Kalman , $H_{\inf}$ and Nonlinear Approaches" ,John Wiley and Sons,New york, 2006.

[28] P. Kundur, "Power system stability and control", 10th reprint, Tata McGraw-Hill Edition, India, 2010.

[29] Z. Huang, K. Schnieder and Jarek Neiplocha,"Feasibility studies of Kalman filter techniques to power system dynamic state estimation", Proc. 8th International Power Engineering Conference IPEC China, pp. 376–382, 2007.

[30] A. Jain and N.R.Shivakumar, "Impact of PMU in dynamic state estimation of power systems", Proc. 40th North American power symposium, NAPS 08,Calgary,AB,Canada, pp.1–8, 2008. DOI: 10.1109/NAPS.2008.5307352

[31] A. Jain and N.R.Shivakumar, "Power system tracking and dynamic state estimation", Proc. Power system conference and exposition, pp. 1-8, 2009. DOI: 10.1109/PSCE.2009.4840192

[32] Siddharth Deshmukh, Balasubramaniam Natarajan and Anil Pahwa, "Stochastic State Estimation for Smart Grids in the Presence of Intermittent Measurements", IEEE Latin-

America Conference on Communications (LATINCOM), pp. 1–6, 2012. DOI: 10.1109/LATINCOM.2012.6506013.

[33] Cem Bila,"Power system dynamic state estimation and load modelling", MS thesis,Northeastern University,Boston, MA, 2014.

[34] US-Canada power system outage task force , "Final report on the August 14th blackout in United States and Canada", Tech Rep.,2004.

[35] R.D.Christie,"Power System Test Archive", http://www.ee.washington.edu/research/pstcs.

[36] N.Sreekanth and Dr M.N.GiriPrasad. Comparative BER Analysis of Mitigation of ICI Through SC,Ml and EKF Methods in OFDM Systems. *International Journal of Electronics and Communication Engineering & Technology (IJECET),* 3 (2), 2012, pp. 69–86.